BGE Research Report No. 04-01

Building Geoenvironment Engineering Laboratory
Department of Urban and Environmental Engineering
Kyoto University
Sakyo, Kyoto 606-8501, Japan

Three-Dimensional Quasi-Static Frictional Contact by using Second-Order Cone Linear Complementarity Problem

Y. Kanno,[†] J.A.C. Martins[‡] and A. Pinto da Costa[§]

February 2004

Abstract A new formulation is presented for the three-dimensional incremental quasi-static problems with unilateral frictional contact. Under the assumptions of small rotations and small strains, a Second-Order Cone Linear Complementarity Problem (SOCLCP) is formulated, which consists of complementarity conditions defined by bilinear functions and conic inequalities. The equilibrium configurations are obtained by using a combined smoothing and regularization method for the second-order cone complementarity problem.

Keywords: contact problem, Coulomb friction, second-order cone, complementarity problem, symmetric cone

[†] Department of Urban and Environmental Engineering, Kyoto University
e-mail: is.kanno@archi.kyoto-u.ac.jp

[‡] Instituto Superior Técnico, Dep. Eng. Civil and ICIST, Av. Rovisco Pais, 1049-001 Lisboa, Portugal
e-mail: jmartins@civil.ist.utl.pt

[§] Instituto Superior Técnico, Dep. Eng. Civil and ICIST, Av. Rovisco Pais, 1049-001 Lisboa, Portugal
e-mail: apcosta@civil.ist.utl.pt

1 Introduction

Various mathematical formulations [2, 3, 1], as well as numerical approaches [5, 4], have been proposed for finite-dimensional frictional contact problems. However, these problems still present some difficulties, both from mathematical and algorithmic points of view. This paper is concerned with quasi-static problems in which finite-dimensional elastic structures may establish frictional contact with the surface of rigid obstacles. Small rotations and small strains are assumed. We consider the classical three-dimensional Coulomb friction law explicitly without any polyhedral approximation.

It is well-known that the two-dimensional (or planar) frictional contact problem can be formulated as a *linear complementarity problem* (*LCP*) [6]. If a polyhedral approximation of the Coulomb friction cone [7] is used, an LCP formulation for the corresponding three-dimensional problem is also classical [8]. Zhang *et al.* [9] proposed a parametric quadratic programming approach for the three-dimensional problem, which also uses the polyhedral approximation. Few studies [10, 13, 4, 12, 11], however, have explicitly dealt with the Coulomb friction law in the three-dimensional space, without any modification. Glocker [10] formulated the nonlinear complementarity problem for a rigid-body frictional contact problem. Garrido *et al.* [4] proposed a numerical method based on the boundary element method, where the Newton–Raphson method is employed at each load increment to determine the correct sliding direction. Strömberg [12] solved three-dimensional fretting problems by using the nonsmooth Newton method, which was also used by Johansson and Klarbring [13] in three-dimensional frictional impact problems. Christensen and Pang [11] proposed the semismooth Newton method for three-dimensional frictional contact problems.

The conventional complementarity formulation of the two-dimensional Coulomb friction law consists of a complementarity condition and some inequality constraints. It is well-known that linear inequalities are used to express the two-dimensional Coulomb friction cone. Indeed, the set of admissible reactions can be transformed into the nonnegative quadrant by rotation with appropriate linear transformation [8]. The constraints on the kinematic variables are also written as linear inequalities, if we assume small deformations and rigid obstacles. Consequently, in the complementarity formulation of the two-dimensional Coulomb friction law, only the complementarity condition is a nonlinear constraint. It should be also emphasized that the complementarity condition can be formulated as a bilinear equation with some auxiliary variables [8].

One of the major difficulties of the three-dimensional frictional contact problems is that the Coulomb friction law itself is expressed as a nonlinear inequality that is nondifferentiable in the ordinary sense. Consequently, the complementarity condition also involves, at least nonlinear [7], and possibly nonsmooth functions [10], if we use the conventional approach for variational inequalities. From the mechanical point of view, this difficulty arises from the constraint that the tangential reaction should be parallel to the incremental tangential displacement, which is a nonconvex and nonsmooth constraint.

In this paper, we propose a novel mathematical and numerical approach for the three-dimensional Coulomb friction law without polyhedral approximations. In contrast with the well-known fact that the formulation for the three-dimensional friction law involves a nondifferentiable complementarity condition, it is rather surprising that the friction law can be expressed by a complementarity condition in a bilinear form over two equivalent convex cones, which is referred to as a *second-order cone linear complementarity problem* (*SOCLCP*). The SOCLCP can be regarded as the natural extension

of the LCP, and is a particular case of a *semidefinite linear complementarity problem* (*SDLCP*) [14]. SOCLCP and SDLCP were introduced as the natural extensions of the *second-order cone programming* (*SOCP*) and the *semidefinite programming* (*SDP*) problems, respectively, and have received increasing attention from mathematical and algorithmic points of view [15, 14, 16]. Although it is well-known that SOCP and SDP have many applications to control theory, engineering, combinatorial optimization, etc. [19, 18, 17, 20, 21, 22], few studies have been published with applications of SOCLCP and SDLCP [23] that cannot be reformulated as convex optimization problems.

One of the reasons why SOCP and SDP have received larger attention is that the efficient algorithms, the so-called *primal-dual interior-point methods* [24, 25], have been proposed for these problems, and there exist several implementations of these algorithms that are well developed [26]. The primal-dual interior-point methods were first proposed for the *linear programming* (*LP*) problem, and were naturally extended to the SDP problem [24]. For SOCP, the primal-dual interior-point methods were developed in a similar manner to those for SDP, by introducing the Euclidean Jordan algebra on second-order cones [25]. Recently, on the basis of the same algebra, the smoothing and regularization methods, which are well-known algorithmic approaches to the nonlinear complementarity problems, have been naturally extended to the *second-order cone complementarity problem* (*SOCCP*) [15, 16].

This paper is organized as follows. We introduce the SOCLCP in Section 2. In Section 3, we formulate the Coulomb friction law as an SOCLCP. The SOCLCP for the incremental quasi-static frictional contact problem is presented in Section 4. In Section 5, the equilibrium configurations as well as the reactions are obtained by solving the proposed SOCLCP problem by using a combined smoothing and regularization method for SOCLCP [15]. Some remarks are presented in Section 6, where our approach is compared with others in the literature, from the unified view point of the Lagrangian for the problem of maximizing the incremental friction dissipation. It is also clarified how our approach can avoid the nonsmoothness and the non-differentiability of the complementarity conditions.

In Sections 5.1 and 5.2, we present 2 examples of application of the proposed method to two-dimensional finite element problems. These examples are a preliminary indispensable and positive test to the proposed formulation. The computational accuracy of the proposed method is compared with that of the Gauss–Seidel method [27]. It should be noted also that the implementation of the proposed methodology is quite independent of the fact that the problem and the friction law are two- or three-dimensional. Sections 5.3 and 5.4 are devoted to the numerical examples, which show the effectiveness of the proposed method in three-dimensional problems. Equilibrium configurations are computed for trusses with various sizes in order to see that the problem size does not affect the computational time of the proposed method drastically.

2 Outline of SOCLCP

Throughout the paper, all vectors are assumed to be column vectors. However, for vectors $\boldsymbol{p} \in \mathbf{R}^n$ and $\boldsymbol{q} \in \mathbf{R}^m$, we often write

$$(\boldsymbol{p}, \boldsymbol{q}) = (\boldsymbol{p}^\top, \boldsymbol{q}^\top)^\top \in \mathbf{R}^{n+m}$$

in order to simplify the notation. We often use the notation $\boldsymbol{x} \cdot \boldsymbol{y}$ for the inner product of $\boldsymbol{x} = (x_i) \in \mathbf{R}^n$ and $\boldsymbol{y} = (y_i) \in \mathbf{R}^n$; i.e.,

$$\boldsymbol{x} \cdot \boldsymbol{y} = \boldsymbol{x}^\top \boldsymbol{y} = \sum_{i=1}^{n} x_i y_i.$$

For any vector $\boldsymbol{p} \in \mathbf{R}^n$, we denote the standard Euclidean norm by $\|\boldsymbol{p}\| = (\boldsymbol{p}^\top \boldsymbol{p})^{1/2}$.

Let $\mathcal{K} \subset \mathbf{R}^n$ denote a closed convex cone. $\mathcal{K}^* \subset \mathbf{R}^n$ denotes the dual cone of $\mathcal{K}$ defined by [28]

$$\mathcal{K}^* = \{\boldsymbol{y} \in \mathbf{R}^n | \boldsymbol{x}^\top \boldsymbol{y} \geq 0 \ (\boldsymbol{x} \in \mathcal{K})\}.$$

We say that $\mathcal{K}$ is *self-dual* if $\mathcal{K} = \mathcal{K}^*$ holds [24]. For a given affine subspace $\mathcal{F}$ of $\mathbf{R}^{2n}$ and a given $\mathcal{K} \subset \mathbf{R}^n$, we consider the following complementarity problem:

$$\left.\begin{array}{ll} \text{find} & (\boldsymbol{x}, \boldsymbol{y}) \in \mathbf{R}^{2n} \\ \text{s.t.} & (\boldsymbol{x}, \boldsymbol{y}) \in \mathcal{F}, \quad \boldsymbol{x} \in \mathcal{K}, \quad \boldsymbol{y} \in \mathcal{K}^*, \quad \boldsymbol{x}^\top \boldsymbol{y} = 0, \end{array}\right\} \tag{1}$$

which is referred to as a *linear complementarity problem over cones* (*LCP over cones*) [29].

Let $\mathbf{R}^n_+ \subset \mathbf{R}^n$ and $\mathbf{L}^n_+ \subset \mathbf{R}^n$ denote the non-negative orthant and *second-order* (or *Lorentz*, or *ice-cream*) *cone* [24], respectively, which are defined as

$$\mathbf{R}^n_+ = \{\boldsymbol{x} = (x_1, \ldots, x_n) \in \mathbf{R}^n | x_i \geq 0 \ (i = 1, \ldots, n)\},$$
$$\mathbf{L}^n_+ = \{\boldsymbol{x} = (x_0, \boldsymbol{x}_1) \in \mathbf{R}^n | x_0 \geq \|\boldsymbol{x}_1\|\}.$$

Let g denote an element of the group G of isomorphisms of the cone $\mathcal{K}$, where the action of g on an interior point $\boldsymbol{t}_1$ of $\mathcal{K}$ is denoted by $g : \boldsymbol{t}_1 \mapsto \tilde{\boldsymbol{t}}_1(g)$. We say that the cone $\mathcal{K}$ is homogeneous if there exists a g satisfying $\tilde{\boldsymbol{t}}_1(g) = \boldsymbol{t}_2$ for any interior points $\boldsymbol{t}_1$ and $\boldsymbol{t}_2$ of $\mathcal{K}$. A homogeneous and self-dual cone is referred to as a *symmetric cone* [30]. For example, any cone that can be expressed via the direct product of a finite number of $\mathbf{R}^n_+$ and $\mathbf{L}^n_+$ is known to be a symmetric cone. Since the symmetric cone is self-dual, the LCP over cones (1) is reduced to

$$\left.\begin{array}{ll} \text{find} & (\boldsymbol{x}, \boldsymbol{y}) \in \mathbf{R}^{2n} \\ \text{s.t.} & (\boldsymbol{x}, \boldsymbol{y}) \in \mathcal{F}, \quad \boldsymbol{x} \in \mathcal{K}, \quad \boldsymbol{y} \in \mathcal{K}, \quad \boldsymbol{x}^\top \boldsymbol{y} = 0, \end{array}\right\} \tag{2}$$

which is referred to as a *linear complementarity problem over symmetric cones* (*LCP over symmetric cones*).

It is well known that the LCP over symmetric cones (2) includes various kinds of complementarity problems as well as optimization problems, which have important applications to engineering, control, finance, combinatorial optimization, etc. Evidently, the LCP [29] is regarded as a special case of the LCP over symmetric cones (2) with $\mathcal{K} = \mathbf{R}^n_+$. If we take $\mathcal{K}$ as the cone of all real symmetric $n \times n$ positive-semidefinite matrices, the LCP over symmetric cones (2) is reduced to the SDLCP [14]. The special class of SDLCP is well-known as the SDP problem [24], which has various fields of application [22, 31, 20]. Moreover, the primal-dual interior-point methods for LP have been naturally extended to SDP [14, 24].

In this paper, we deal with the special class of LCP over symmetric cones (2) for which $\mathcal{K} \subset \mathbf{R}^n$ can be written as

$$\mathcal{K} = \mathcal{K}_{\mathrm{S}} := \mathcal{K}_1 \times \cdots \times \mathcal{K}_k, \quad \mathcal{K}_i = \mathbf{R}^{n_i}_+ \text{ or } \mathbf{L}^{n_i}_+,$$

where $n = \sum_{i=1}^{k} n_i$. For the given $\boldsymbol{M} \in \mathbf{R}^{n\times n}$ and $\boldsymbol{q} \in \mathbf{R}^n$, we may take

$$\mathcal{F} = \{(\boldsymbol{x}, \boldsymbol{y}) \in \mathbf{R}^{2n} | \boldsymbol{y} = \boldsymbol{M}\boldsymbol{x} + \boldsymbol{q}\}.$$

Then the LCP over symmetric cones (2) is reduced to

$$\left.\begin{array}{ll} \text{find} & (\boldsymbol{x}, \boldsymbol{y}) \in \mathbf{R}^{2n} \\ \text{s.t.} & \boldsymbol{y} = \boldsymbol{M}\boldsymbol{x} + \boldsymbol{q}, \\ & \boldsymbol{x} \in \mathcal{K}_{\mathrm{S}}, \quad \boldsymbol{y} \in \mathcal{K}_{\mathrm{S}}, \quad \boldsymbol{x}^{\top}\boldsymbol{y} = 0, \end{array}\right\} \tag{3}$$

which is referred to as the *second-order cone linear complementarity problem* (*SOCLCP*).

Observing that $\mathbf{L}_{+}^{1} = \mathbf{R}_{+}^{1}$, we can easily see that the SOCLCP (3) has the LCP as a particular case. Moreover, the SOCLCP is important because the necessary and sufficient conditions for optimality of an SOCP problem can be written as an SOCLCP, under the generalized Slater's constraint qualification [25]. Recently, one of the authors proposed SOCP formulations for large-deformation analysis of cable networks [17] with contact conditions [18] as well as with the minimum principle of complementary energy [19]. Since the SOCLCP is a special class of the SDLCP, the theory and algorithms developed for the SDLCP can be immediately applied to the SOCLCP. However, it is not recommended to solve the SOCLCP by reformulating it as an SDLCP (see, e.g., Alizadeh and Goldfarb [25] for the case of SOCP and SDP). Based on the Euclidean Jordan algebra on second-order cones [25], Hayashi *et al.* [15] proposed an algorithm that uses smoothing and regularization methods. The smoothing functions associated with SOCCP were proposed by Chen *et al.* [32] and Chen *et al.* [16].

3 Complementarity formulation of friction law

In this section, the Coulomb friction law is formulated as a linear complementarity condition over two second-order cones.

Consider a contact candidate node in three-dimensional space. For each contact candidate node, we may consider a reference frame $(\boldsymbol{t}_1, \boldsymbol{t}_2, \boldsymbol{n})$ such that $\boldsymbol{n} \in \mathbf{R}^3$ and $\boldsymbol{t}_1,\ \boldsymbol{t}_2 \in \mathbf{R}^3$ are normal and tangential, respectively, to the corresponding surface of the obstacle. Let $(\Delta\boldsymbol{u}_{\mathrm{t}}, \Delta u_{\mathrm{n}}) \in \mathbf{R}^2 \times \mathbf{R}$ and $(\boldsymbol{r}_{\mathrm{t}}, r_{\mathrm{n}}) \in \mathbf{R}^2 \times \mathbf{R}$ denote the vector of incremental displacements and the vector of reactions, respectively. Here, the subscripts 't' and 'n' denote the quantities with respect to the frame $(\boldsymbol{t}_1, \boldsymbol{t}_2)$ and the axis $\boldsymbol{n}$, respectively. Letting $\mu > 0$ denote the constant coefficient of friction and assuming

$$r_{\mathrm{n}} \geq 0, \tag{4}$$

the classical Coulomb friction law can be written as

$$\begin{cases} \Delta\boldsymbol{u}_{\mathrm{t}} = \boldsymbol{0} \Longrightarrow \mu r_{\mathrm{n}} \geq \|\boldsymbol{r}_{\mathrm{t}}\| & \text{(stick condition)}, \\ \Delta\boldsymbol{u}_{\mathrm{t}} \neq \boldsymbol{0} \Longrightarrow \boldsymbol{r}_{\mathrm{t}} = -\mu r_{\mathrm{n}} \dfrac{\Delta\boldsymbol{u}_{\mathrm{t}}}{\|\Delta\boldsymbol{u}_{\mathrm{t}}\|} & \text{(slip condition)}. \end{cases} \tag{5}$$

The following lemma plays a key role in our formulation of Section 4:

Lemma 3.1. $\Delta \boldsymbol{u}_{\mathrm{t}} \in \mathbf{R}^2$ *and* $(\boldsymbol{r}_{\mathrm{t}}, r_{\mathrm{n}}) \in \mathbf{R}^2 \times \mathbf{R}$ *satisfy* (4) *and* (5) *if and only if there exists a* $\lambda_{\mathrm{n}} \in \mathbf{R}$ *satisfying*

$$\beta = (\lambda_{\mathrm{n}}, \Delta \boldsymbol{u}_{\mathrm{t}}) \cdot (\mu r_{\mathrm{n}}, \boldsymbol{r}_{\mathrm{t}}) = 0, \tag{6}$$

$$\lambda_{\mathrm{n}} \geq \|\Delta \boldsymbol{u}_{\mathrm{t}}\|, \quad \mu r_{\mathrm{n}} \geq \|\boldsymbol{r}_{\mathrm{t}}\|. \tag{7}$$

Lemma 3.1 can be proved similarly to the proof of Theorem 4.3 in Kanno and Ohsaki [19]. However, to make this paper self-contained, we give the independent proof presented next.

Proof of Lemma 3.1. The 'only if' part is immediately proved by substituting (5) and $\lambda_{\mathrm{n}} = \|\Delta \boldsymbol{u}_{\mathrm{t}}\|$ into (6) and (7). For the 'if' part, it follows from (6) and (7) that

$$\beta \geq (\|\Delta \boldsymbol{u}_{\mathrm{t}}\|, \Delta \boldsymbol{u}_{\mathrm{t}}) \cdot (\mu r_{\mathrm{n}}, \boldsymbol{r}_{\mathrm{t}}) \geq 0. \tag{8}$$

On the other hand, it is known [33](§ 5.2.1) that $\Delta \boldsymbol{u}_{\mathrm{t}}$, $\boldsymbol{r}_{\mathrm{t}}$ and r_{n} satisfy (4) and (5) if and only if $\mu r_{\mathrm{n}} \geq \|\boldsymbol{r}_{\mathrm{t}}\|$ and $(\|\Delta \boldsymbol{u}_{\mathrm{t}}\|, \Delta \boldsymbol{u}_{\mathrm{t}}) \cdot (\mu r_{\mathrm{n}}, \boldsymbol{r}_{\mathrm{t}}) = 0$ hold. The statement of Lemma 3.1 follows immediately from this and (8). □

An alternative proof of Lemma 3.1 is given in Section 6. It should be emphasized that the Coulomb friction law is expressed as a linear complementarity condition over two second-order cones in the three-dimensional space. In order to show that the proposed formulation is independent of the concepts addressed earlier in the literature, we compare in Section 6 the formulation in the system (6) and (7) with others in the literature.

Remark 3.2. Observe that $r_{\mathrm{n}} \geq 0$ holds if (6) and (7) are satisfied. It follows immediately from the proof of Lemma 3.1 and $\mu > 0$ that λ_{n} satisfies

$$\lambda_{\mathrm{n}} = \|\Delta \boldsymbol{u}_{\mathrm{t}}\| \quad (\text{if } r_{\mathrm{n}} > 0), \tag{9}$$

$$\lambda_{\mathrm{n}} \geq \|\Delta \boldsymbol{u}_{\mathrm{t}}\| \quad (\text{if } r_{\mathrm{n}} = 0), \tag{10}$$

if (6) and (7) are satisfied. It should be emphasized that (9) and (10) provide the physical interpretation of the auxiliary variable λ_{n}; i.e., for $r_{\mathrm{n}} > 0$, λ_{n} coincides with the norm of increment of tangential displacement at each contact node. Suppose $r_{\mathrm{n}} > 0$ in (6) and (7). Then the condition (6) is rewritten as

$$\lambda_{\mathrm{n}}(-\mu r_{\mathrm{n}}) = \Delta \boldsymbol{u}_{\mathrm{t}}^{\top} \boldsymbol{r}_{\mathrm{t}}. \tag{11}$$

From (7) and (9), it is easily seen that the left-hand side of (11) is reduced to $-\|\Delta \boldsymbol{u}_{\mathrm{t}}\|\|\boldsymbol{r}_{\mathrm{t}}\|$; i.e., both the left- and the right-hand sides of (11) correspond to the incremental work done by friction. □

Remark 3.3. It is well-known that various kinds of convex sets defined by nonlinear nonsmooth functions can be expressed via a finite number of second-order cones [24]. For example, it is easy to see that the ellipsoidal friction law [7] can also be formulated as linear complementarity conditions over second-order cones by using the linear transformation. □

4 SOCLCP formulation

We consider finite-dimensional elastic structures in the three-dimensional space possibly in contact with some rigid obstacles. We assume small rotations and small strains, and investigate the quasi-static frictional contact problem. The set of contact candidate nodes is appropriately specified [34].

Let n^{d} denote the number of degrees of freedom. $\widehat{\boldsymbol{u}}^0 \in \mathbf{R}^{n^{\mathrm{d}}}$ and $\widehat{\boldsymbol{r}}^0 \in \mathbf{R}^{n^{\mathrm{d}}}$ denote the known vectors of nodal displacements and reactions at the equilibrium state associated with the specified external forces $\widehat{\boldsymbol{f}}^0_{\mathrm{ext}} \in \mathbf{R}^{n^{\mathrm{d}}}$; i.e.,

$$\widehat{\boldsymbol{K}}\widehat{\boldsymbol{u}}^0 = \widehat{\boldsymbol{f}}^0_{\mathrm{ext}} + \widehat{\boldsymbol{r}}^0 \tag{12}$$

holds, where $\widehat{\boldsymbol{K}} \in \mathbf{R}^{n^{\mathrm{d}}} \times \mathbf{R}^{n^{\mathrm{d}}}$ denotes the symmetric stiffness matrix. Let n^{c} denote the number of contact candidate nodes. n^{F} denotes the number of degrees of freedom that are not associated to contact, i.e., $n^{\mathrm{F}} = n^{\mathrm{d}} - 3n^{\mathrm{c}}$. Hereafter, the superscripts C and F refer to the nodes that are associated and not associated to contact, respectively. Any variable preceded by Δ corresponds to the increment of that variable. The incremental form of equilibrium equations (12) reads

$$\widehat{\boldsymbol{K}}\Delta\widehat{\boldsymbol{u}} = \Delta\widehat{\boldsymbol{f}}_{\mathrm{ext}} + \Delta\widehat{\boldsymbol{r}}, \tag{13}$$

where

$$\widehat{\boldsymbol{K}} = \begin{pmatrix} \boldsymbol{K}^{\mathrm{FF}} & \boldsymbol{K}^{\mathrm{FC}} \\ \boldsymbol{K}^{\mathrm{CF}} & \boldsymbol{K}^{\mathrm{CC}} \end{pmatrix}, \quad \Delta\widehat{\boldsymbol{u}} = \begin{pmatrix} \Delta\boldsymbol{u}^{\mathrm{F}} \\ \Delta\boldsymbol{u}^{\mathrm{C}} \end{pmatrix}, \quad \Delta\widehat{\boldsymbol{f}}_{\mathrm{ext}} = \begin{pmatrix} \Delta\boldsymbol{f}^{\mathrm{F}}_{\mathrm{ext}} \\ \Delta\boldsymbol{f}^{\mathrm{C}}_{\mathrm{ext}} \end{pmatrix}, \quad \Delta\widehat{\boldsymbol{r}} = \begin{pmatrix} \boldsymbol{0} \\ \Delta\boldsymbol{r}^{\mathrm{C}} \end{pmatrix}.$$

The normal nodal gap g^0_i is specified for each $i = 1, \ldots, n^{\mathrm{c}}$, which indicates the current gap between the ith node and the corresponding obstacle surface. For each $i = 1, \ldots, n^{\mathrm{c}}$, let $r^{\mathrm{C}}_{\mathrm{n}i} \in \mathbf{R}$ and $\boldsymbol{r}^{\mathrm{C}}_{\mathrm{t}i} \in \mathbf{R}^2$, respectively, denote the normal reaction and the tangential reaction vector for the ith contact candidate node. We write $\boldsymbol{r}^{\mathrm{C}}_{\mathrm{n}} = (r^{\mathrm{C}}_{\mathrm{n}1}, \ldots, r^{\mathrm{C}}_{\mathrm{n}n^{\mathrm{c}}}) \in \mathbf{R}^{n^{\mathrm{c}}}$, $\boldsymbol{r}^{\mathrm{C}}_{\mathrm{t}} = (\boldsymbol{r}^{\mathrm{C}}_{\mathrm{t}1}, \ldots, \boldsymbol{r}^{\mathrm{C}}_{\mathrm{t}n^{\mathrm{c}}}) \in \mathbf{R}^{2n^{\mathrm{c}}}$ and $\boldsymbol{r}^{\mathrm{C}} = (\boldsymbol{r}^{\mathrm{C}}_{\mathrm{t}}, \boldsymbol{r}^{\mathrm{C}}_{\mathrm{n}}) \in \mathbf{R}^{3n^{\mathrm{c}}}$. In a similar manner, $\Delta u^{\mathrm{C}}_{\mathrm{n}i} \in \mathbf{R}$, $\Delta\boldsymbol{u}^{\mathrm{C}}_{\mathrm{t}i} \in \mathbf{R}^2$, $\Delta\boldsymbol{u}^{\mathrm{C}}_{\mathrm{n}} \in \mathbf{R}^{n^{\mathrm{c}}}$ and $\Delta\boldsymbol{u}^{\mathrm{C}}_{\mathrm{t}} \in \mathbf{R}^{2n^{\mathrm{c}}}$ are defined, where $\Delta\boldsymbol{u}^{\mathrm{C}} = (\Delta\boldsymbol{u}^{\mathrm{C}}_{\mathrm{t}}, \Delta\boldsymbol{u}^{\mathrm{C}}_{\mathrm{n}}) \in \mathbf{R}^{3n^{\mathrm{c}}}$. The classical Signorini contact conditions are formulated as [7]

$$\Delta u^{\mathrm{C}}_{\mathrm{n}i} - g^0_i \geq 0, \quad r^{\mathrm{C}}_{\mathrm{n}i} \geq 0, \quad (\Delta u^{\mathrm{C}}_{\mathrm{n}i} - g^0_i) r^{\mathrm{C}}_{\mathrm{n}i} = 0 \quad (i = 1, \ldots, n^{\mathrm{c}}). \tag{14}$$

For simplicity, we write

$$\begin{aligned} &\Delta u_{\mathrm{n}i} = \Delta u^{\mathrm{C}}_{\mathrm{n}i} - g^0_i, \quad \Delta\boldsymbol{u}_{\mathrm{t}i} = \Delta\boldsymbol{u}^{\mathrm{C}}_{\mathrm{t}i}, \quad \Delta\boldsymbol{u} = (\Delta\boldsymbol{u}_{\mathrm{t}1}, \ldots, \Delta\boldsymbol{u}_{\mathrm{t}n^{\mathrm{c}}}, \Delta u_{\mathrm{n}1}, \ldots, \Delta u_{\mathrm{n}n^{\mathrm{c}}}), \\ &r_{\mathrm{n}i} = r^{\mathrm{C}}_{\mathrm{n}i}, \quad \boldsymbol{r}_{\mathrm{t}i} = \boldsymbol{r}^{\mathrm{C}}_{\mathrm{t}i}, \quad \boldsymbol{r} = \boldsymbol{r}^{\mathrm{C}}. \end{aligned}$$

Then (14) is reduced to

$$\Delta u_{\mathrm{n}i} \geq 0, \quad \Delta r_{\mathrm{n}i} \geq 0, \quad \Delta u_{\mathrm{n}i} r_{\mathrm{n}i} = 0 \quad (i = 1, \ldots, n^{\mathrm{c}}), \tag{15}$$

Define the symmetric matrix $\boldsymbol{K} \in \mathbf{R}^{3n^{\mathrm{c}} \times 3n^{\mathrm{c}}}$ and the vector $\boldsymbol{f} \in \mathbf{R}^{3n^{\mathrm{c}}}$ as

$$\begin{aligned} &\boldsymbol{K} = \boldsymbol{K}^{\mathrm{CC}} - \boldsymbol{K}^{\mathrm{CF}}(\boldsymbol{K}^{\mathrm{FF}})^{-1}\boldsymbol{K}^{\mathrm{FC}}, \\ &\boldsymbol{f} = \boldsymbol{r}^{0\mathrm{C}} + \Delta\boldsymbol{f}^{\mathrm{C}}_{\mathrm{ext}} + \boldsymbol{K}^{\mathrm{CF}}(\boldsymbol{K}^{\mathrm{FF}})^{-1}\Delta\boldsymbol{f}^{\mathrm{F}}_{\mathrm{ext}} - \boldsymbol{K}\boldsymbol{g}^0, \end{aligned}$$

where $\boldsymbol{K}$ and $\boldsymbol{f}$ are constant, $\boldsymbol{g}^0 = (\boldsymbol{0}, g_1^0, \ldots, g_{n^{\mathrm{c}}}^0) \in \mathbf{R}^{3n^{\mathrm{c}}}$ and $\widehat{\boldsymbol{r}}^0 = (\boldsymbol{0}, \boldsymbol{r}^{0^{\mathrm{C}}})^\top \in \mathbf{R}^{n^{\mathrm{F}}} \times \mathbf{R}^{3n^{\mathrm{c}}}$. Then (13) is reduced to the following equilibrium equations only in terms of the kinematic and static variables of the contact candidate nodes:

$$\boldsymbol{K}\Delta\boldsymbol{u} = \boldsymbol{r} + \boldsymbol{f}. \tag{16}$$

It follows from (15), (16) and Lemma 3.1 that the equilibrium state $(\Delta\boldsymbol{u}, \boldsymbol{r})$ is obtained as the solution to the following problem:

$$\left.\begin{array}{ll} \text{find} & (\Delta\boldsymbol{u}, \boldsymbol{r}, \boldsymbol{\lambda}_{\mathrm{n}}) \in \mathbf{R}^{3n^{\mathrm{c}}} \times \mathbf{R}^{3n^{\mathrm{c}}} \times \mathbf{R}^{n^{\mathrm{c}}} \\ \text{s.t.} & \boldsymbol{K}\Delta\boldsymbol{u} = \boldsymbol{r} + \boldsymbol{f}, \\ & \Delta u_{\mathrm{n}i} \geq 0, \quad r_{\mathrm{n}i} \geq 0, \quad \Delta u_{\mathrm{n}i} r_{\mathrm{n}i} = 0 \quad (i = 1, \ldots, n^{\mathrm{c}}), \\ & \lambda_{\mathrm{n}i} \geq \|\Delta\boldsymbol{u}_{\mathrm{t}i}\|, \quad \mu r_{\mathrm{n}i} \geq \|\boldsymbol{r}_{\mathrm{t}i}\|, \\ & \qquad (\lambda_{\mathrm{n}i}, \Delta\boldsymbol{u}_{\mathrm{t}i}) \cdot (\mu r_{\mathrm{n}i}, \boldsymbol{r}_{\mathrm{t}i}) = 0 \quad (i = 1, \ldots, n^{\mathrm{c}}), \end{array}\right\} \tag{17}$$

which is an SOCLCP. Define $\mathcal{K}_1 \subset \mathbf{R}^{3n^{\mathrm{c}}}$ as

$$\mathcal{K}_1 = \{(\boldsymbol{s}_1, \boldsymbol{s}_2) \in \mathbf{R}^{n^{\mathrm{c}}} \times \mathbf{R}^{2n^{\mathrm{c}}} | s_{1i} \geq \|\boldsymbol{s}_{2i}\| \ (i = 1, \ldots, n^{\mathrm{c}})\}, \tag{18}$$

where $\boldsymbol{s}_1 = (s_{11}, \ldots, s_{1n^{\mathrm{c}}})$, $\boldsymbol{s}_2 = (\boldsymbol{s}_{21}, \ldots, \boldsymbol{s}_{1n^{\mathrm{c}}})$ and $\boldsymbol{s}_{2i} \in \mathbf{R}^2$ $(i = 1, \ldots, n^{\mathrm{c}})$. Observe that (16) is decomposed as

$$\begin{pmatrix} \boldsymbol{K}_{\mathrm{t}} \\ \boldsymbol{K}_{\mathrm{n}} \end{pmatrix} \Delta\boldsymbol{u} = \begin{pmatrix} \boldsymbol{r}_{\mathrm{t}} \\ \boldsymbol{r}_{\mathrm{n}} \end{pmatrix} + \begin{pmatrix} \boldsymbol{f}_{\mathrm{t}} \\ \boldsymbol{f}_{\mathrm{n}} \end{pmatrix},$$

where $\boldsymbol{K}_{\mathrm{t}} \in \mathbf{R}^{2n^{\mathrm{c}} \times 3n^{\mathrm{c}}}$, $\boldsymbol{K}_{\mathrm{n}} \in \mathbf{R}^{n^{\mathrm{c}} \times 3n^{\mathrm{c}}}$, $\boldsymbol{f}_{\mathrm{t}} \in \mathbf{R}^{2n^{\mathrm{c}}}$ and $\boldsymbol{f}_{\mathrm{n}} \in \mathbf{R}^{n^{\mathrm{c}}}$. By putting

$$\boldsymbol{x} = \begin{pmatrix} \boldsymbol{\lambda}_{\mathrm{n}} \\ \Delta\boldsymbol{u}_{\mathrm{t}} \\ \Delta\boldsymbol{u}_{\mathrm{n}} \end{pmatrix}, \quad \boldsymbol{y} = \begin{pmatrix} \mu\boldsymbol{r}_{\mathrm{n}} \\ \boldsymbol{r}_{\mathrm{t}} \\ \boldsymbol{r}_{\mathrm{n}} \end{pmatrix}, \quad \mathcal{K}_{\mathrm{S}} = \mathcal{K}_1 \times \mathbf{R}_+^{n^{\mathrm{c}}},$$
$$\boldsymbol{M} = \begin{pmatrix} \boldsymbol{O} & \mu\boldsymbol{K}_{\mathrm{n}} \\ \boldsymbol{O} & \boldsymbol{K} \end{pmatrix}, \quad \boldsymbol{q} = \begin{pmatrix} -\mu\boldsymbol{f}_{\mathrm{n}} \\ -\boldsymbol{f} \end{pmatrix}, \quad n = 4n^{\mathrm{c}},$$

we see that the Problem (17) is embedded into the standard form of the SOCLCP (3).

Remark 4.1. Consider the case of two-dimensional problem of the SOCLCP (17). Since the second-order cone $\mathbf{L}_+^2 = \{(x_0, x_1) \in \mathbf{R}^2 | x_0 \geq |x_1|\}$ is a rotation of the nonnegative quadrant, it is clear that the SOCLCP (17) is reduced to a generalized LCP in the sense of [29]. □

5 Examples

In order to obtain the equilibrium configuration as well as the reactions in frictional contact problems, the SOCLCP (17) is solved by using the algorithm proposed by Hayashi *et al.* [15], which is a smoothing and regularization method based on the Euclidean Jordan algebra on second-order cones [30, 25]. All the algorithmic parameters are assigned the values used by Hayashi *et al.* [15] in the numerical examples in [15], where the initial solution is assigned as $\boldsymbol{x}^0 = \boldsymbol{y}^0 = \boldsymbol{0}$. Computation has been carried out on Pentium III (844MHz) with 256MB of memory running Windows XP, using MATLAB Version 6.5 [35].

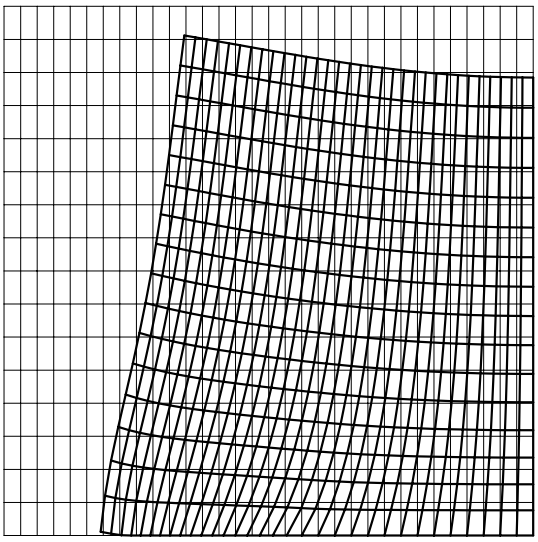

Figure 1: Deformed configuration of the elastic square body at an equilibrium state corresponding to a rightward pressure of 100 MPa on the left face and a downward pressure of 50 MPa on the segment CD (displacements amplified 500 times).

5.1 A linear elastic square body in plane strain submitted to distributed forces.

We consider the well-known example in the literature [37, 36]. It consists of a linear elastic body (Young's modulus $E = 130$ GPa, Poisson's ratio $\nu = 0.2$) in a state of plane strain occupying a 40 mm $\times$ 40 mm square domain as illustrated in Fig.1. The self-weight is neglected. The solid is discretized in 512 bilinear (Q1) finite elements. The right boundary is in an axis of symmetry, where only one of half part is illustrated in Fig.1, hence the nodes on that boundary are constrained to move only in the vertical direction. The nodes of the bottom segment are submitted to frictional contact conditions with $\mu = 1$. The left and top boundary segments are submitted to a monotonic proportional loading that consists of 100 MPa rightward and 50 MPa downward uniform stresses, respectively. The contact stresses are represented in Fig.2 and match the results presented in [37, 36]; the tangential reaction stresses point to the right.

5.2 A linear elastic square body against an inclined obstacle.

In this example we study an 80 mm $\times$ 80 mm isotropic linear elastic square ($E = 5$ MPa, $\nu = 0.4$) in plane strain, in the presence of an inclined plane obstacle, as illustrated in Fig.3. The self-weight of the block is not considered. The boundary segment CD is submitted to the following prescribed rigid body motion: a first downward movement of 0.7 mm followed by a succession of 0.05 mm leftward *horizontal* prescribed displacements. For simplicity, and only for the purpose of testing the algorithm, we consider the downward movement of 0.7 mm in a single step. The nodes on the segment AB may establish contact with the obstacle. At the unstressed initial state, node B is in contact with zero reaction and the distance between node A and the obstacle is 1 mm. The coefficient of friction between the obstacle and the each node on the segment AB is $\mu = 0.5$. The square is discretized with a uniform mesh of 50×50 bilinear (Q1) finite elements, where $n^{\mathrm{c}} = 51$.

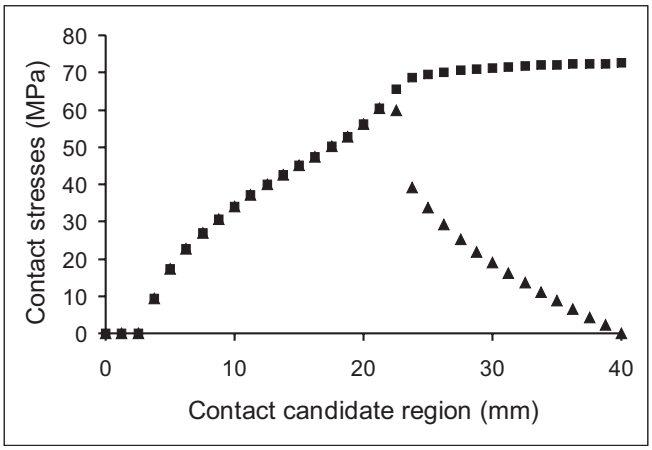

Figure 2: Schematic representation of the normal contact stresses $r_{\mathrm{n}i}$ (■) and the tangential contact stresses divided by the coefficient of friction $r_{\mathrm{t}i}/\mu$ (▲) for the equilibrium state corresponding to the configuration represented in Fig.1.

Fig.4 illustrates the equilibrium configuration when the horizontal displacement of segment CD is $11 \times 0.05 = 0.55$ mm to the left, where the nodes in stick and free conditions are indicated by ∘ and •, respectively. All the remaining nodes are in slipping contact. Table 1 contains the absolute displacements and the nodal contact reactions as well as the frictional contact state for 6 contact candidate nodes indicated in Fig.4, obtained by the proposed method for the same equilibrium state. The blocked node 51 (B) has a positive absolute tangential displacement because in previous load increments the node B did slip to the right. In Fig.5 we observe that the tangential stresses of the right part of the contact region point towards the left in spite of the fact that the segment CD has already suffered a 0.55 mm horizontal displacement to the left: this is due to the Poisson effect associated to the initial downward movement of the segment CD; in Fig.5, negative tangential contact stresses correspond to a reaction tangential stress vector in the direction of $-\boldsymbol{t}$, where $\boldsymbol{t}$ is defined in Fig.3. A very good agreement is obtained between the results of the proposed method and those obtained with a block Gauss–Seidel algorithm [27].

With the increase of the prescribed horizontal displacement of the segment CD, the number of blocked nodes decreases and the number of nodes in impending slip to the left increases. After an horizontal prescribed movement of $22 \times 0.05 = 1.1$ mm there exists no blocked node; the corresponding contact stresses are illustrated in Fig.6.

It is interesting to note that the effective contact region increases between the equilibrium state corresponding to a 0.55 mm horizontal displacement of the segment CD (Fig.5) and the equilibrium state corresponding to a 1.1 mm horizontal displacement of the segment CD (Fig.6), although the prescribed relative movement (horizontal to the left) of the segment CD between the two equilibrium states drives the block away from the obstacle. This effect is due to the friction stresses exerted on the bottom of the block towards the right, which cause a counterclockwise rotation and consequent approach towards the obstacle of the left (still out of contact) part of the contact candidate region AB.

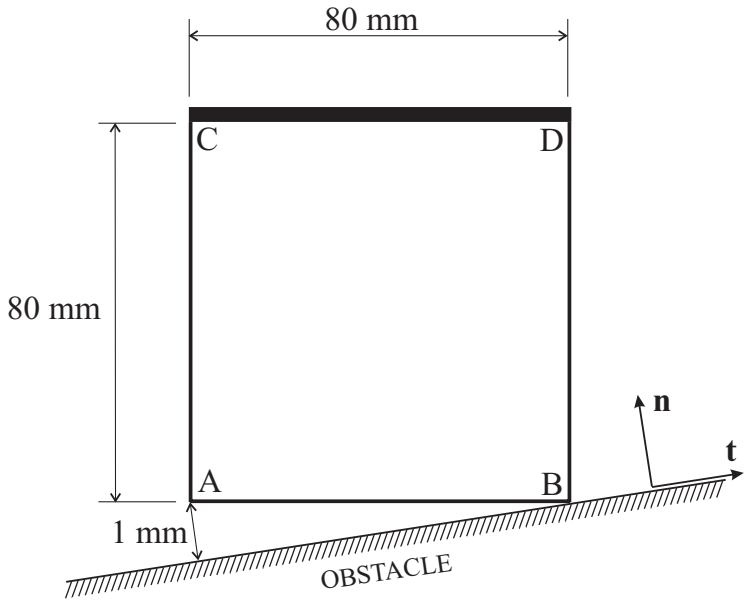

Figure 3: Schematic representation of a square block that may establish contact with an inclined plane obstacle.

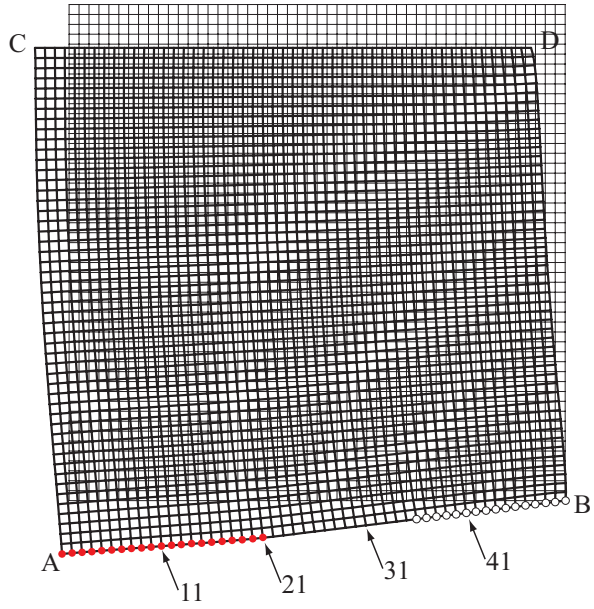

Figure 4: Deformed configuration of the square block at the equilibrium state corresponding to a 0.7 mm downward prescribed displacement followed by a $11 \times 0.05 = 0.55$ mm leftward horizontal prescribed displacement of the upper face (displacements amplified 10 times).

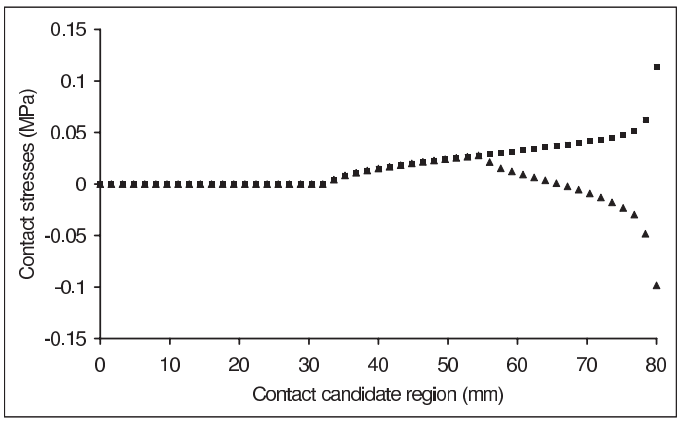

Figure 5: Schematic representation of the normal contact stresses $r_{\mathrm{n}i}$ (■) and the tangential contact stresses divided by the coefficient of friction $r_{\mathrm{t}i}/\mu$ (▲) for the equilibrium state corresponding to the configuration represented in Fig.4.

Table 1: Solution of the quasi–static incremental problem corresponding to a 0.7 mm downward prescribed displacement followed by a $11 \times 0.05 = 0.55$ mm leftward horizontal prescribed displacement of the upper face (equilibrium state represented in Fig.4). The second column contains the frictional contact state: o = out of contact, $s-$ = impending slip to the left, b = blocked.

node	state	Δu_{n}	Δu_{t}	r_{n}	r_{t}
$1 \equiv \mathrm{A}$	o	$0.85805 \times 10^{+00}$	$-.12437 \times 10^{+00}$	$.3154 \times 10^{-12}$	0.7541×10^{-13}
11	o	$0.73384 \times 10^{+00}$	$-.11919 \times 10^{+00}$	$.6768 \times 10^{-12}$	$-.3358 \times 10^{-12}$
21	o	$0.59913 \times 10^{+00}$	$-.83151 \times 10^{-01}$	$.3895 \times 10^{-10}$	0.8548×10^{-09}
31	$s-$	$0.40000 \times 10^{+00}$	$-.16279 \times 10^{-01}$	$.3652 \times 10^{-01}$	0.1826×10^{-01}
41	b	$0.20000 \times 10^{+00}$	$-.48565 \times 10^{-14}$	$.5695 \times 10^{-01}$	0.2822×10^{-02}
$51 \equiv \mathrm{B}$	b	$-.49175 \times 10^{-12}$	0.57589×10^{-02}	$.9106 \times 10^{-01}$	$-.3938 \times 10^{-01}$

Table 2: Results of double-layer grids.

model	n^{c}	n	$\mathcal{K}_{\mathrm{S}}$	#iter	cpu(s)	err_1	err_2
4×4	16	64	$(\mathbf{R}_+ \times \mathbf{L}_+^3)^{16}$	10	0.93	−1.3-12	−1.3-12
7×7	49	196	$(\mathbf{R}_+ \times \mathbf{L}_+^3)^{49}$	13	9.22	−4.1-13	−4.1-13
10×10	100	400	$(\mathbf{R}_+ \times \mathbf{L}_+^3)^{100}$	11	33.40	−1.3-13	−1.3-13
12×12	144	484	$(\mathbf{R}_+ \times \mathbf{L}_+^3)^{144}$	10	79.41	−1.8-13	−1.8-13

5.3 Double-layer grids.

Equilibrium configurations as well as reactions are found for four double-layer trusses with 4×4, 7×7, 10×10 and 12×12 grids, with a single loading step. The cases of 4×4 and 7×7 grids are shown in Fig.7. The lengths of the members in the x- and y-directions are 2000.0 mm and 3000.0 mm, respectively, and the distance between the upper and lower planes is 2000.0 mm. The elastic modulus and the cross-sectional area for each member are given as $E = 205.8$ GPa and $a_j = 10000.0$ mm^2, respectively. However, E and a_j are scaled so that $E = 1000.0$ and $a_j = 0.01$ are satisfied. The external loads $\widehat{\boldsymbol{f}} = (82.32, 41.16, -82.32)$ kN are applied at the each node indicated

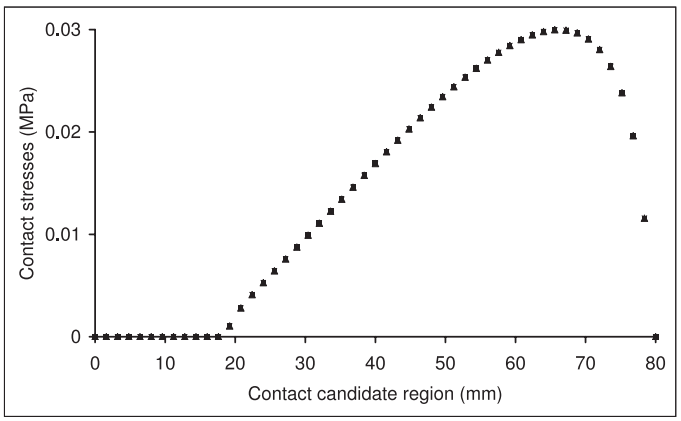

Figure 6: Schematic representation of the normal contact stresses $r_{\mathrm{n}i}$ (■) and the tangential contact stresses divided by the coefficient of friction $r_{\mathrm{t}i}/\mu$ (▲) at an equilibrium state corresponding to a 0.7 mm downward prescribed displacement followed by a $22 \times 0.05 = 1.1$ mm leftward horizontal prescribed displacement of the segment CD.

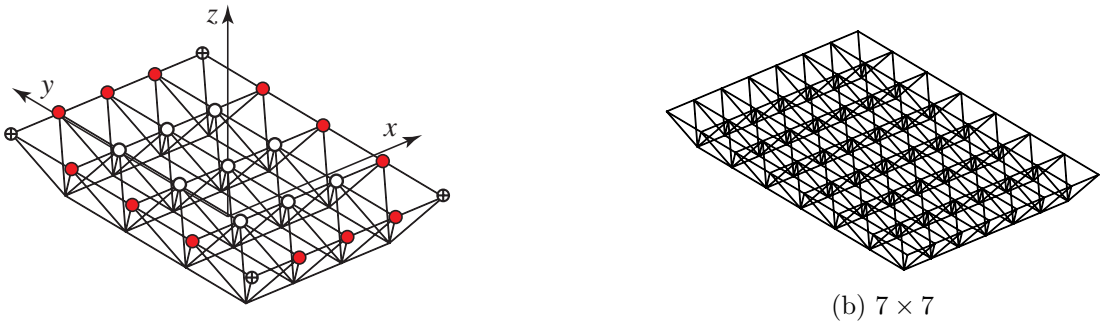

(a) 4×4

(b) 7×7

Figure 7: Double-layer grids.

by $\circ$ in Fig.7 (a). $\widehat{\boldsymbol{f}}/2$ and $\widehat{\boldsymbol{f}}/4$, respectively, are applied at nodes indicated by $\bullet$ and $\oplus$. All nodes belonging to the lower layer are pin-supported, which possibly contact with the rigid obstacle defined by $\{(x, y, z) \in \mathbf{R}^3 | z \leq 0\}$. We specify the reference state of each truss such that there exists no initial gap between each support and the surface of obstacle, i.e., $g_i^0 = 0$ $(i = 1, \ldots, n^{\mathrm{c}})$ and no external forces are applied. The coefficient of friction is specified as $\mu = 1.5$ at each contact candidate node. Consequently, the geometry, distribution of stiffness, support conditions, initial gap and coefficients of friction of these trusses are all symmetric with respect to xz- and yz-planes.

The results obtained are listed in Table 2, where #iter denotes the number of Newton iterations, i.e., the total number of inner iterations of Algorithm 4.1 in [15], and cpu(s) denotes the total CPU time for solving the SOCLCP (17) in seconds. In accordance with Mittelmann [26], we define two error measures err_1 and err_2 related to complementarity conditions by

$$\mathrm{err}_1 = \frac{\boldsymbol{x}^\top \boldsymbol{y}}{1 + \boldsymbol{x}^\top \boldsymbol{y}}, \quad \mathrm{err}_2 = \frac{\boldsymbol{x}^\top (\boldsymbol{M}\boldsymbol{x} + \boldsymbol{q})}{1 + \boldsymbol{x}^\top \boldsymbol{y}}.$$

It is observed in Table 2 that each of the solutions satisfies the complementarity conditions with high accuracy. The algorithm does not find any difficulty in computing an equilibrium solution for each case. It may be observed in Table 2 that the CPU time is of an order between n^2 and n^3, which

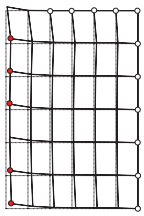

(a) 7×7 double-layer grid ($\times 20$).

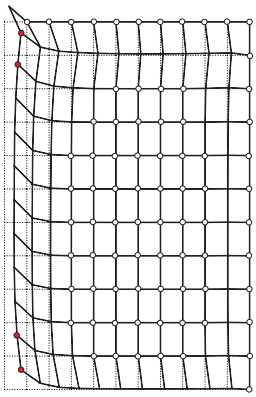

(b) 12×12 double-layer grid ($\times 100$).

Figure 8: Displacements of contact candidate nodes.

Table 3: Definitions of $\gamma^{(m)}$s.

m	0	1	2	3	4	5	6
$\gamma^{(m)}$	0	5.00	4.05	3.10	2.15	1.20	0.25

Table 4: Results of incremental problems of 12×12 grids.

m	#iter	cpu(s)	err_1	err_2
1	8	63.3	−5.0-12	−5.0-12
2	7	55.7	−1.3-16	−1.3-16
3	7	55.5	−9.8-16	−9.8-16
4	7	55.5	−1.6-15	−1.6-15
5	9	73.0	−1.1-12	−1.1-12
6	13	106.1	−1.1-14	−1.1-14

implies that the problem size does not affect the CPU time drastically.

The displacements of the contact candidate nodes for the 7×7 and 12×12 grids at the obtained equilibrium configurations are illustrated in Fig.8, where the nodes in stick and free conditions are indicated by $\circ$ and $\bullet$, respectively. All the remaining nodes are in slipping contact. It is interesting to observe in Fig.8 that almost all nodes along the north- and the east-ends of each truss are in stick, which agrees with the well-known property of frictional contact problems for continua.

5.4 Incremental problem of 12×12 double-layer grid.

The quasi-static incremental problem is solved for the 12×12 double-layer grid truss defined in Section 5.3. Take $\mu = 0.12$. The distribution of external forces is given in a manner similar to the case of Section 5.3. Letting $\Delta\widehat{\boldsymbol{f}} = (0, 0, -102.9)$ kN, consider the 6 loading steps such that $\widehat{\boldsymbol{f}}$ for each increment is specified as

$$\widehat{\boldsymbol{f}} = \gamma^{(m)} \Delta\widehat{\boldsymbol{f}} \quad (m = 0, \ldots, 6), \tag{19}$$

where $\gamma^{(m)}$s are listed in Table 3; i.e., at the increments $m = 2, \ldots, 6$, the external forces applied at $m = 1$ are monotonically removed. Note that the equilibrium configuration of this example does

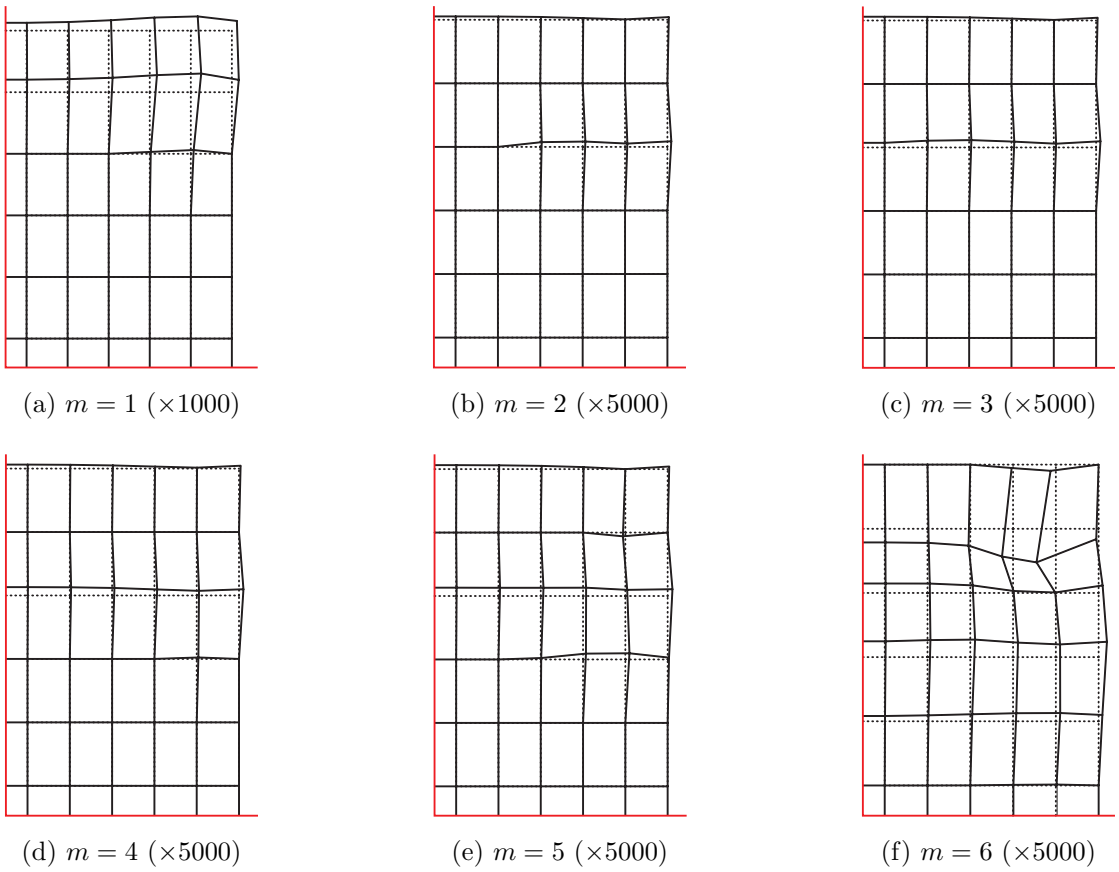

(a) $m = 1$ ($\times 1000$) (b) $m = 2$ ($\times 5000$) (c) $m = 3$ ($\times 5000$)

(d) $m = 4$ ($\times 5000$) (e) $m = 5$ ($\times 5000$) (f) $m = 6$ ($\times 5000$)

Figure 9: Increments of displacements of contact candidate nodes.

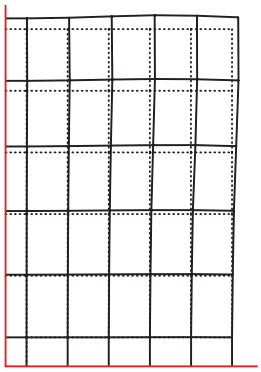

Figure 10: Total displacements of contact candidate nodes at $m = 6$ ($\times 1000$).

not change drastically if we choose smaller step sizes during the loading process.

The results obtained are listed in Table 4. At each increment the algorithm finds a solution without any difficulty. It is observed in Table 4 that the solutions obtained satisfy the frictional contact conditions with high accuracy. For each $i = 1, \ldots, m$, the incremental displacements of the contact candidate nodes are shown in Fig.9, where only one of four equal parts is shown, due to symmetry. All contact candidate nodes are in contact at every increment. The equilibrium configuration obtained at $m = 6$ is illustrated in Fig.10.

Notice here that, in the definition (19) of the external forces $\widehat{\boldsymbol{f}}$, there exists no equilibrium configuration if we take $\gamma^{(m)} < 0$. For $\gamma^{(m)} = 0$, any configuration without member elongations, allowing rigid-body motion satisfying $\Delta u_{\mathrm{n}i} \geq 0$ $(i = 1, \ldots, n^{\mathrm{c}})$, solves (17). It should be emphasized that the equilibrium solution is found without difficulty for $m = 6$, even if $\gamma^{(6)}$ is considerably small.

In the literature of incremental frictional contact problems, the example of removing the applied external loads from a flat punch on elastic foundation was investigated for axisymmetric case in [38]. Klarbring [8] solved the same problem for rectangular punch numerically with polyhedral friction cone. The example investigated in this section has some similarity with that of [8], because, at the start of unloading, some contact nodes slip in the same directions as those during loading. More relevant studies are listed in [8].

6 Remarks on Lagrangian and cone complementarity

We start with an alternative proof of Lemma 3.1, which is based on the maximal dissipation law [7] and the KKT conditions for the linear programming problem over symmetric cones [24].

The friction law introduced in (4) and (5) can be alternatively derived from the maximal dissipation law [39, 7]; i.e., the tangential reaction $\boldsymbol{r}_{\mathrm{t}} \in \mathbf{R}^2$ is given as an optimal solution of the following problem in variables $\boldsymbol{r}'_{\mathrm{t}} \in \mathbf{R}^2$:

$$\left.\begin{array}{rll} \boldsymbol{r}_{\mathrm{t}} \in & \underset{\boldsymbol{r}'_{\mathrm{t}} \in \mathbf{R}^2}{\operatorname{argmin}} & \Delta \boldsymbol{u}_{\mathrm{t}}^{\top} \boldsymbol{r}'_{\mathrm{t}} \\ & \text{s.t.} & \mu r_{\mathrm{n}} \geq \|\boldsymbol{r}'_{\mathrm{t}}\|. \end{array}\right\} \tag{20}$$

Evidently, we may assume $\mu r_{\mathrm{n}} \geq 0$, i.e., the Problem (20) is feasible. We shall show that the complementarity conditions (6) and (7) are naturally induced from the optimality conditions of the Problem (20).

Alternative proof of Lemma 3.1. The Lagrangian $L_1 : \mathbf{R}^4 \mapsto (-\infty, +\infty]$ of the Problem (20) in variables $(\boldsymbol{r}'_{\mathrm{t}}, \boldsymbol{\lambda})$ with $\boldsymbol{\lambda} = (\lambda_{\mathrm{n}}, \boldsymbol{\lambda}_{\mathrm{t}}) \in \mathbf{R} \times \mathbf{R}^2$ is defined as

$$L_1(\boldsymbol{r}'_{\mathrm{t}}, \boldsymbol{\lambda}) = \begin{cases} \Delta \boldsymbol{u}_{\mathrm{t}}^{\top} \boldsymbol{r}'_{\mathrm{t}} - \lambda_{\mathrm{n}}(\mu r_{\mathrm{n}}) - \boldsymbol{\lambda}_{\mathrm{t}}^{\top} \boldsymbol{r}'_{\mathrm{t}} & (\lambda_{\mathrm{n}} \geq \|\boldsymbol{\lambda}_{\mathrm{t}}\|), \\ +\infty & (\text{otherwise}). \end{cases} \tag{21}$$

Indeed, by using the self-duality of a second-order cone, i.e.,

$$\mu r_{\mathrm{n}} \geq \|\boldsymbol{r}'_{\mathrm{t}}\| \Longleftrightarrow \lambda_{\mathrm{n}}(\mu r_{\mathrm{n}}) + \boldsymbol{\lambda}_{\mathrm{t}}^{\top} \boldsymbol{r}'_{\mathrm{t}} \geq 0, \quad \forall (\lambda_{\mathrm{n}}, \boldsymbol{\lambda}_{\mathrm{t}}),\ \lambda_{\mathrm{n}} \geq \|\boldsymbol{\lambda}_{\mathrm{t}}\|,$$

we see that the Problem (20) is equivalent to the following problem:

$$\min_{\boldsymbol{r}'_{\mathrm{t}} \in \mathbf{R}^2} \quad \sup\{L_1(\boldsymbol{r}'_{\mathrm{t}}, \boldsymbol{\lambda}) | \boldsymbol{\lambda} \in \mathbf{R}^3\}, \tag{22}$$

which validates that L_1 can be regarded as the (extended) Lagrangian of the Problem (20) (see, e.g., Rockafellar [28]).

Note that the Problem (20) is an SOCP problem. It follows from the (generalized) KKT conditions (Ekeland and Temám [40, Proposition VI 2.2]) that $\boldsymbol{r}'_{\mathrm{t}} \in \mathbf{R}^2$ is a global optimal solution

of the Problem (20) if and only if there exists a Lagrange multiplier $\boldsymbol{\lambda} \in \mathbf{R}^3$ satisfies the following conditions:

$$\mu r_{\mathrm{n}} \geq \|\boldsymbol{r}'_{\mathrm{t}}\|, \quad \lambda_{\mathrm{n}} \geq \|\boldsymbol{\lambda}_{\mathrm{t}}\|, \tag{23}$$

$$\beta_1 = \lambda_{\mathrm{n}}(\mu r_{\mathrm{n}}) + \boldsymbol{\lambda}_{\mathrm{t}}^{\top} \boldsymbol{r}'_{\mathrm{t}} = 0, \tag{24}$$

$$\frac{\partial L_1}{\partial \boldsymbol{r}'_{\mathrm{t}}} = \Delta \boldsymbol{u}_{\mathrm{t}} - \boldsymbol{\lambda}_{\mathrm{t}} = \mathbf{0}. \tag{25}$$

Substitution of (25) into (23) shows that the KKT conditions (23)–(25) are equivalent to (6) and (7). □

Note that L_1 defined by (21) is continuously differentiable at any point $(\boldsymbol{r}'_{\mathrm{t}}, \boldsymbol{\lambda}) \in \mathrm{int}(\mathrm{dom}\, L_1)$. Alternatively, in the context of the conventional nonlinear programming approach [41], the Lagrangian $L_2 : \mathbf{R}^3 \mapsto (-\infty, +\infty]$ of the Problem (20) is defined as

$$L_2(\boldsymbol{r}'_{\mathrm{t}}, \lambda_2) = \begin{cases} \Delta \boldsymbol{u}_{\mathrm{t}}^{\top} \boldsymbol{r}'_{\mathrm{t}} - \lambda_2(\mu r_{\mathrm{n}} - \|\boldsymbol{r}'_{\mathrm{t}}\|) & (\lambda_2 \geq 0), \\ +\infty & (\text{otherwise}), \end{cases} \tag{26}$$

where $\lambda_2 \in \mathbf{R}$ is the Lagrangian multiplier. Here, L_2 defined by (26) is not differentiable in the ordinary sense at several interior points of the effective domain of L_2. By using L_2, the following optimality conditions of the Problem (20) are obtained:

$$\mu r_{\mathrm{n}} - \|\boldsymbol{r}'_{\mathrm{t}}\| \geq 0, \quad \lambda_2 \geq 0, \tag{27}$$

$$\beta_2 = \lambda_2(\mu r_{\mathrm{n}} - \|\boldsymbol{r}'_{\mathrm{t}}\|) = 0, \tag{28}$$

$$\Delta \boldsymbol{u}_{\mathrm{t}} \|\boldsymbol{r}'_{\mathrm{t}}\| + \lambda_2 \boldsymbol{r}'_{\mathrm{t}} = \mathbf{0}, \tag{29}$$

where (29) is derived from the stationary condition of L_2 with respect to $\boldsymbol{r}'_{\mathrm{t}}$.

In the sense of the frictional contact problem, $\boldsymbol{r}_{\mathrm{n}}$, $\Delta \boldsymbol{u}_{\mathrm{t}}$ and λ_2 are also considered as variables in the system (27)–(29). Observe that the inequalities of (27) are convex. It should be emphasized that, in the complementarity condition (28), β_2 is nonsmooth and nonconvex with respect to $\boldsymbol{r}'_{\mathrm{t}}$. Moreover, the stationary condition (29) of L_2 is also a nonsmooth and nonconvex constraint with respect to $(\boldsymbol{r}'_{\mathrm{t}}, \Delta \boldsymbol{u}_{\mathrm{t}}, \lambda_2)$, since L_2 is a nonsmooth function on $\mathrm{int}(\mathrm{dom}\, L_2)$. Hence, it is not easy to solve the system (27)–(29) directly. This explains, from the view point of the Lagrangian, that the conventional complementarity formulation is not recommended for three-dimensional frictional contact problem.

Klarbring and Pang [7] and Christensen and Pang [11] considered the following formulation of maximal dissipation law:

$$\left.\begin{array}{rll} \boldsymbol{r}_{\mathrm{t}} \in & \underset{\boldsymbol{r}'_{\mathrm{t}} \in \mathbf{R}^2}{\mathrm{argmin}} & \Delta \boldsymbol{u}_{\mathrm{t}}^{\top} \boldsymbol{r}'_{\mathrm{t}} \\ & \text{s.t.} & \mu^2 r_{\mathrm{n}}^2 - \boldsymbol{r}_{\mathrm{t}}'^{\top} \boldsymbol{r}'_{\mathrm{t}} \geq 0, \end{array}\right\} \tag{30}$$

which is a convex quadratic programming problem. The Lagrangian $L_3 : \mathbf{R}^3 \mapsto (-\infty, +\infty]$ of the Problem (30) is defined as

$$L_3(\boldsymbol{r}'_{\mathrm{t}}, \lambda_3) = \begin{cases} \Delta \boldsymbol{u}_{\mathrm{t}}^{\top} \boldsymbol{r}'_{\mathrm{t}} - \lambda_3(\mu^2 r_{\mathrm{n}}^2 - \boldsymbol{r}_{\mathrm{t}}'^{\top} \boldsymbol{r}'_{\mathrm{t}}) & (\lambda_3 \geq 0), \\ +\infty & (\text{otherwise}), \end{cases} \tag{31}$$

where $\lambda_3 \in \mathbf{R}$ is the Lagrange multiplier. Compared with L_2, L_3 defined by (31) seems to have the advantage that it is continuously differentiable at any point $(\boldsymbol{r}'_{\mathrm{t}}, \lambda_3) \in \mathrm{int}(\mathrm{dom}\, L_3)$. Consequently, the following KKT conditions are easily derived:

$$\mu^2 r_{\mathrm{n}}^2 - \boldsymbol{r}_{\mathrm{t}}'^{\top} \boldsymbol{r}'_{\mathrm{t}} \geq 0, \quad \lambda_3 \geq 0, \tag{32}$$

$$\beta_3 = \lambda_3 (\mu^2 r_{\mathrm{n}}^2 - \boldsymbol{r}_{\mathrm{t}}'^{\top} \boldsymbol{r}'_{\mathrm{t}}) = 0, \tag{33}$$

$$\frac{\partial L_3}{\partial \boldsymbol{r}'_{\mathrm{t}}} = \Delta \boldsymbol{u}_{\mathrm{t}} + 2\lambda_3 \boldsymbol{r}'_{\mathrm{t}} = \boldsymbol{0}. \tag{34}$$

Consider $\boldsymbol{r}'_{\mathrm{t}}$, r_{n}, $\Delta \boldsymbol{u}_{\mathrm{t}}$ and λ_3 as variables in the system (32)–(34). The inequality constraints (32) are convex again. In the complementarity condition of (33), β_3 is smooth, which may be regarded as a 'nice' property. However, β_3 is convex and nonconvex quadratic function, respectively, with respect to r_{n} and $\boldsymbol{r}'_{\mathrm{t}}$. Moreover, the stationary condition (34) is also nonconvex. By eliminating λ_3 from (33) and (34), we obtain

$$\mu r_{\mathrm{n}} \Delta \boldsymbol{u}_{\mathrm{t}} + \| \Delta \boldsymbol{u}_{\mathrm{t}} \| \boldsymbol{r}'_{\mathrm{t}} = \boldsymbol{0}. \tag{35}$$

Consequently, we may solve the system (32) and (35). Unfortunately, the condition (35) is again nonsmooth.

We shall revisit the proposed system (23)–(25). Consider $\boldsymbol{r}'_{\mathrm{t}}$, r_{n}, $\Delta \boldsymbol{u}_{\mathrm{t}}$, λ_{n} and $\boldsymbol{\lambda}_{\mathrm{t}}$ as variables. It should be emphasized that (i) the inequality constraints of (23) are convex; (ii) in the complementarity condition (24), β_1 is linear with respect to $\boldsymbol{r}'_{\mathrm{t}}$, r_{n}, λ_{n} and $\boldsymbol{\lambda}_{\mathrm{t}}$; (iii) the stationary condition (25) is linear. The 'nice' properties (i)–(iii) explain the advantage of the proposed formulation compared with those discussed above. From the view point of the Lagrangian, the properties (i)–(iii) are achieved since L_1 defined by (21) is linear function with respect to $(\boldsymbol{r}'_{\mathrm{t}}, r_{\mathrm{n}}, \Delta \boldsymbol{u}_{\mathrm{t}}, \boldsymbol{\lambda})$ at any point $(\boldsymbol{r}'_{\mathrm{t}}, \boldsymbol{\lambda}) \in \mathrm{dom}\, L_1$. This is rather surprising because the Problem (20) is nonlinear. It should be emphasized that we can formulate L_1 with the properties (i)–(iii) by utilizing the self-dual property of second-order cones [24]. For an engineering application of this type of Lagrangian, see [19, 18]. It is also interesting to see that the difference between various formulations of the friction conditions can be interpreted on the basis of the Lagrangian of the maximal dissipation law. From the mechanical point of view, the conditions (29) and (34) (or (35)) imply that the tangential reaction $\boldsymbol{r}_{\mathrm{t}}$ should be parallel to the incremental tangential displacements $\Delta \boldsymbol{u}_{\mathrm{t}}$, which is an essentially nonlinear constraint (see, e.g., [10]). This may be one of major difficulties in three-dimensional frictional contact problems. However, the proposed system (23)–(25) does not have this constraint explicitly, which explains its advantage.

7 Conclusions

An SOCLCP formulation has been presented for the incremental quasi-static three-dimensional frictional contact problem, without any modification of the Coulomb friction law. It should be emphasized that the proposed formulation provides an unified methodology both for two- and three-dimensional friction laws. In numerical examples, it has been shown that the equilibrium configuration can be obtained as a solution of the SOCLCP by using a combined smoothing and regularization method. Since the complementarity condition is expressed via a smooth bilinear function, the equilibrium configuration can be obtained without any difficulty. Existing formulations for

three-dimensional frictional contact problems in the literature have been compared from the unified view point of Lagrangian duality.

Acknoledgement

The authors are grateful to Prof. M. Fukushima and Mr. S. Hayashi (Kyoto University, Japan) for having allowed the use of the software developed by them, which is an implementation of the algorithm proposed in [15].

References

[1] Mijar AR, Arora JS. Review of formulations for elastostatic frictional contact problems. *Struct. Multidisc. Optim.* 2000; **20**:167–189.

[2] Outrata J, Kočvara M, Zowe J. *Nonsmooth Approach to Optimization with Equilibrium Constraints.* Kluwer Academic Publishers: Netherlands, 1998.

[3] Pang J-S, Stewart DE. A unified approach to discrete frictional contact problems. *Int. J. Engrg. Sci.* 1999; **37**:1747–1768.

[4] Garrido JA, Foces A, Paŕis F. An incremental procedure for three-dimensional contact problems with friction. *Comput. & Struct.* 1994; **50**:201–215.

[5] Wang Y-C, Lakes R. Analytical parametric analysis of the contact problem of human buttocks and negative Poisson's ratio foam cushions. *Int. J. Solids Struct.* 2002; **39**:4825–4838.

[6] Christensen PW. A semi-smooth Newton method for elasto-plastic contact problem. *Int. J. Solids Struct.* 2002; **39**:2323–2341.

[7] Klarbring A, Pang J-S. Existence of solutions to discrete semicoercive frictional contact problems. *SIAM J. Optim.* 1998; **8**:414–442.

[8] Klarbring A. A mathematical programming approach to three-dimensional contact problems with friction. *Comp. Methods Appl. Mech. Engrg.* 1986; **58**:175–200.

[9] Zhang H, Zhong W, Gu Y. A combined parametric quadratic programming and iteration method for 3-D elastic-plastic frictional contact problem analysis. *Comp. Methods Appl. Mech. Engrg.* 1998; **155**:307–324.

[10] Glocker C. Formulation of spatial contact situations in rigid multibody systems. *Comp. Methods Appl. Mech. Engrg.* 1999; **177**:199–214.

[11] Christensen PW, Pang J-S. Frictional contact algorithms based on semismooth Newton methods. In *Reformulation—Nonsmooth, Piecewise Smooth, Semismooth and Smoothing Methods,* Fukushima M, Qi L (eds). Kluwer Academic Publishers: Boston, MA, 1999; 81–116.

[12] Strömberg N. A Newton method for three-dimensional fretting problems. *Int. J. Solids Struct.* 1999; **36**:2075-2090.

[13] Johansson L, Klarbring A. Study of frictional impact using a nonsmooth equations solver. *J. Appl. Mech. (ASME)* 2000; **67**:267–273.

[14] Kojima M, Shindoh S, Hara S. Interior-point methods for the monotone semidefinite linear complementarity problems. *SIAM J. Optim.* 1997; **7**:86–125.

[15] Hayashi S, Yamashita N, Fukushima M. A combined smoothing and regularization method for monotone second-order cone complementarity problems, *Technical Report 2003-002,* Department of Applied Mathematics and Physics, Kyoto University, February, 2003.

[16] Chen XD, Sun D, Sun J. Complementarity functions and numerical experiments on some smoothing Newton methods for second-order-cone complementarity problems. *Preprint,* Dept. of Mathematics, National University of Singapore, Republic of Singapore, 2002.

[17] Kanno Y, Ohsaki M, Ito J. Large-deformation and friction analysis of nonlinear elastic cable networks by second-order cone programming. *Int. J. Numer. Meth. Engrg.* 2002; **55**:1079–1114.

[18] Kanno Y, Ohsaki M. Second-order cone programming for contact analysis of cable networks. *Proc. of the Fifth World Congress of Structural and Multidisciplinary Optimization (WCSMO5)* Lido di Jesolo, Italy, May 19-23, 2003.

[19] Kanno Y, Ohsaki M. Minimum principle of complementary energy of cable networks by using second-order cone programming *Int. J. Solids Struct.* 2003; **40**:4437–4460.

[20] Kanno Y, Ohsaki M, Katoh N. Sequential semidefinite programming for optimization of framed structures under multimodal buckling constraints. *International Journal of Structural Stability and Dynamics* 2001; **1**:585–602.

[21] Lobo MS, Vandenberghe L, Boyd S, Lebret H. Applications of second-order cone programming. *Linear Algebra and its Applications* 1998; **284**:193–238.

[22] Vandenberghe L, Boyd S. Semidefinite programming. *SIAM Review* 1996; **38**:49–95.

[23] El Ghaoui L, Oustry F, AitRami M. A cone complementarity linearization algorithm for static output-feedback and related problems. *IEEE Trans. Autom. & Control* 1997; **42**.

[24] Ben-Tal A, Nemirovski A. *Lectures on Modern Convex Optimization*: *Analysis, Algorithms, and Engineering Applications.* SIAM: Philadelphia, 2001.

[25] Alizadeh F, Goldfarb D. Second-order cone programming. *Math. Program.* 2003; **B95**:3–51.

[26] Mittelmann HD. An independent benchmarking of SDP and SOCP solvers. *Math. Programming* 2003; **B95**:407–430.

[27] Jourdan F, Alart P, Jean M. A Gauss–Seidel like algorithm to solve frictional contact problems. *Comput. Meth. Appl. Mech. Engrg.* 1998; **155**:31–47.

[28] Rockafellar RT. *Convex Analysis.* Princeton University Press, 1970.

[29] Kojima M, Shida M, Shindoh S. Reduction of monotone linear complementarity problems over cones to linear programs over cones. *Acta Mathematica Vietnamica* 1997; **22**:147–157.

[30] Faraut J, Korányi A. *Analysis on Symmetric Cones.* Oxford University Press, 1994.

[31] Ohsaki M, Fujisawa K, Katoh N, Kanno Y. Semi-definite programming for topology optimization of trusses under multiple eigenvalue constraints. *Comp. Meth. Appl. Mech. Engrg.* 1999; **80**:203–217.

[32] Chen J-S, Chen X, Tseng P. Analysis of nonsmooth vector-valued functions associated with second-order cones. *Manuscript,* Dept. of Mathematics, University of Washington, USA, 2002.

[33] Duvaut G, Lions JL. *Inequalities in Mechanics and Physics.* Springer-Verlag, Berlin, Heiderberg, 1976.

[34] Kikuchi N, Oden JT. *Contact Problem in Elasticity*: *A Study of Variational Inequalities and Finite Element Methods.* SIAM; Philadelphia, 1988.

[35] The MathWorks, Inc. *Using MATLAB.* The MathWorks, Inc., Natick, MA, 1999.

[36] Tin-Loi F, Xia SH. An iterative complementarity approach for elastoplastic analysis involving frictional contact. *Int. J. Mech. Sci.* 2003; **45**:197–216.

[37] Raous M, Chabrand P., Lebon F. Numerical methods for frictional contact problems and applications. *Journal of Theoretical and Applied Mechanics* 1988; Special issue, supplement 1,**7**:111–128.

[38] Torstenfelt BR. An automatic incrementation technique for contact problems with friction. *Computers & Structures* 1984; **19**:393–400.

[39] Pang J-S, Trinkle J. Stability characterizations of rigid body contact problems with Coulomb friction. *ZAMM* 2000; **80**:643–663.

[40] Ekeland I, Temám R. *Convex Analysis and Variational Problems.* North-Holland, Amsterdam, 1976; also: Classics in Applied Mathematics, SIAM, Philadelphia, 1999.

[41] Mangasarian OL. *Nonlinear Programming.* McGraw-Hill, New York, 1969.